Ca^{2+}, Mg^{2+}, Li^+, Na^+, and K^+ Distributions in the Headgroup Region of Binary Membranes of Phosphatidylcholine and Phosphatidylserine As Seen by Deuterium NMR†

Michel Roux*,‡ and Myer Bloom
Department of Physics, University of British Columbia, Vancouver, British Columbia V6T 2A6, Canada
Received February 5, 1990; Revised Manuscript Received April 6, 1990

ABSTRACT: The binding of calcium, magnesium, lithium, potassium, and sodium to membrane bilayers of 5 to 1 (M/M) 1-palmitoyl-2-oleoylphosphatidylcholine (POPC) and 1-palmitoyl-2-oleoylphosphatidylserine (POPS) was investigated by using deuterium nuclear magnetic resonance (^2H NMR). Both lipids were deuteriated on their polar headgroups, and spectra were obtained at 25 °C in the liquid-crystalline phase as a function of salt concentration. The spectra obtained with calcium were correlated with $^{45}CaCl_2$ binding studies to determine the effective membrane-bound calcium at low calcium binding, up to 0.78 calcium per POPS. Deuterium quadrupolar splittings of both POPC and POPS headgroups were shown to be very sensitive to calcium binding. The behavior of these two headgroups over a wide range of $CaCl_2$ concentrations suggests that Ca^{2+} binding occurs in at least two steps, the first step being achieved with 0.5 M $CaCl_2$, with a stoichiometry of 0.5 Ca^{2+} per POPS. Correlations of the deuterium Ca^{2+} binding data with related data obtained after incorporation of a cationic integral peptide showed that the effects of these two cationic molecules on the POPS headgroup are qualitatively similar, and provided further support for two-step Ca^{2+} binding to the POPC/POPS 5:1 membranes. The corresponding data obtained with magnesium, lithium, and potassium indicate that these cations interact with both the choline and serine headgroups. The amplitudes of headgroup perturbations could be partly correlated to the relative affinities of the metallic cations for the lipid membrane. The two-step binding described with Ca^{2+} appears to be relevant to the Mg^{2+} data, and in certain limits to the Li^+ data. The data were interpreted in terms of conformational changes of the lipid headgroups induced by an electric field due to the charges of the membrane-bound metallic cations. A conformational change of the serine headgroup induced by the membrane-bound charges is proposed. We propose that the metallic cations can be differentiated on the basis of their respective spatial distribution functions relative to the choline and serine headgroups. According to this interpretation, the divalent cations Ca^{2+} and Mg^{2+} are more deeply buried in the membrane than monovalent Na^+ and K^+, the case of Li^+ being intermediate of the latter two. This conclusion is discussed in relation to fundamental theories of the spatial distribution of ions near the interface between water and smooth charged solid surfaces.

Metallic cations, particularly calcium, play an important role in the functions of biological membranes. The biological responses induced by the interaction of metallic cations with lipid membranes can be modulated by the properties of the cation and by the chemical composition of the lipid surface, the latter being determined by the nature of the lipid headgroups. The adsorption of metallic cations to lipid membranes, as monitored by classical binding studies, is associated with an increase in the ion concentration at the membrane–solution interface. This "interface" should be actually viewed as a three-dimensional region of space, whose limits can be broadly defined by the polar moieties of the phospholipids, and the contiguous water layers, particularly the first layer containing oriented water molecules [Söderman et al., 1983; see also general theoretical studies of Patey and Torrie (1989)].

Membrane–cation interactions have been extensively studied through their equilibrium binding constant and the stoichiometry of the interaction, which are primarily related to the *quantity* of ions contained in this interface. In this regard, it has been shown that metallic cations display a wide range of affinities for lipid membranes, which can be primarily related to the net charge of the ion in the order tri- > di- > monovalent cations (Eisenberg et al., 1979; McLaughlin et al., 1981; Bentz et al., 1988; Bloch & Yun, 1990). There are up to now few available data concerning the relative *distributions* of membrane-bound cations within the three-dimensional space associated with the membrane–solution interface. The spatial distribution of charges near charged (or uncharged) membrane surfaces is actually a major unsolved theoretical problem in current membrane research. The importance of this problem in relation to understanding forces between membranes, problems of self-assembly of lipids and proteins, and other fundamental biological processes has been reviewed recently by McLaughlin (1989) and Ninham (1989). It seems that in regard to recent theoretical progress done in this field, experimental methods capable of directly probing the interfacial region on a molecular distance scale are now clearly needed.

Deuterium nuclear magnetic resonance (^2H NMR)[1] of headgroup-deuteriated phospholipids has been shown to be sensitive to the adsorption of charged molecules at the mem-

† This work was supported by grants from the Natural Sciences and Engineering Research Council of Canada.
‡ Present address: Département de Biologie, Service de Biophysique, CEN-Saclay, 91191 Gif-sur-Yvette, France.

[1] Abbreviations: NMR, nuclear magnetic resonance; DMPC, 1,2-dimyristoyl-*sn*-glycero-3-phosphocholine; DMPS, 1,2-dimyristoyl-*sn*-glycero-3-phosphoserine; POPC, 1-palmitoyl-2-oleoyl-*sn*-glycero-3-phosphocholine; POPS, 1-palmitoyl-2-oleoyl-*sn*-glycero-3-phosphoserine; PC, phosphatidylcholine; PS, phosphatidylserine; PG, phosphatidylglycerol; HEPES, *N*-(2-hydroxyethyl)piperazine-*N*'-2-ethanesulfonic acid; EDTA, ethylenediaminetetraacetic acid.

0006-2960/90/0429-7077$02.50/0

brane surface. On the basis of studies involving headgroup-deuteriated phosphatidylcholine (PC), Seelig et al. (1987) have developed the idea that the deuterium quadrupolar splittings of the choline moiety act as a molecular electrometer, reflecting the net charge density at the membrane surface. This property of the PC headgroup was related to a charge-induced conformational change of the choline segment evidenced by the ^2H NMR data. Hence, deuterium NMR of headgroup-deuteriated phospholipids provides a direct method for the investigation at the molecular level of the binding of metallic cations to the membrane surface. This approach has been applied to deuteriated PC headgroups, in the course of Ca^{2+} binding studies to pure PC (Altenbach & Seelig, 1984), and PG- and cardiolipin-containing membranes (Macdonald & Seelig, 1987a,b), allowing a discussion of the PC/Ca^{2+} binding equilibrium. Following related studies on PC and phosphatidylserine (PS) headgroup perturbations induced by membrane-bound cationic peptides (Roux et al., 1988, 1989), we have shown that the magnitude and sign of the perturbation to the ^2H NMR quadrupolar splittings of ^2H nuclei in the polar headgroup are also affected by the *location* of the charges relative to the headgroup charge distribution. Thus, it appears that the distribution of metallic cations in lipid bilayers could be probed by ^2H NMR of headgroup-deuteriated phospholipids.

In the present work, ^2H NMR of headgroup-deuteriated phospholipids was used to monitor the interaction of mono- and divalent cations, with both PC and PS headgroups. A detailed study of Ca^{2+} binding to binary membranes of 5:1 (M/M) POPC/POPS is first described, followed by a comparative analysis of related NMR data obtained upon binding of Mg^{2+}, Li^+, K^+, and Na^+ to the same membranes. The overall results provide evidence that the metallic cations investigated can be distinguished by their spatial distribution relative to the lipid headgroups. After a qualitative discussion of the data, we conclude with a discussion of the theoretical implications of the results of our study. This theoretical discussion starts with an extension of an earlier electrostatic model (Roux et al., 1989) describing the interaction of the lipid headgroup charges with an electric field generated by the distribution of the positive charges of the metallic cations. We also discuss connections with fundamental theories of electric fields near smooth interfaces on which progress is being made and finish with a discussion of a possible ion-induced conformational change of the serine headgroup in terms of a model proposed by Scherer and Seelig (1989).

Materials and Methods

Lipids and Peptides. POPA, POPC, and POPS were purchased from Avanti Polar Lipids (Birmingham, AL). Headgroup-deuteriated POPC was prepared by condensing POPA and deuteriated choline bromide (Merck, Sharp & Dohm) as described by Roux et al. (1983). Headgroup-deuteriated POPS was prepared from POPA and perdeuteriated serine according to Browning and Seelig (1980) and Roux and Neumann (1986), and purified on preparative TLC (Merck 5717, 20 cm × 20 cm × 0.5 cm). The following nomenclature is employed for the deuteriation sites of the choline and serine headgroups:

$$\text{PC: } {}^{-}O_3POC\overset{\alpha}{H}_2C\overset{\beta}{H}_2N(CH_3)_3^{+}$$

$$\text{PS: } {}^{-}O_3POC\overset{\alpha}{H}_2C\overset{\beta}{H}(NH_3^{+})COO^{-}$$

The amphiphilic cationic peptide Lys-Lys-Gly-Leu_{20}-Lys-Lys-Ala-$CONH_2$ ($K_2GL_{20}K_2A$) was synthesized according to the method described by Davis et al. (1983).

Sample Preparation. Liposomes were prepared by mixing chloroform solutions of POPC and POPS in a 5:1 molar ratio. The organic solutions were divided in aliquots containing 45 μmol of lipid, and the solvent was removed by evaporation under N_2. The solid residues were dried under vacuum (10^{-2} mmHg) for 12 h and dispersed with continuous vortexing at 40 °C, in 500 μL of Hepes buffer (50 mM in deuterium-depleted water, pH 7.5, and 40 mM NaCl) containing the appropriate concentration of salt, giving 90 mM lipid dispersions. The resulting samples were submitted to five freezing (liquid nitrogen) and thawing (25 °C) cycles and centrifuged at 25 °C (90000 rpm, 2 h), and the resulting pellet was transferred directly into the NMR tubes. In certain cases, the salt concentrations were raised by supplementing the pellets with appropriate amounts of concentrated salt solutions, followed by freezing and thawing of the membranes. The resulting variations in the lipid concentrations were small, except for the lithium data which were brought down to 72 mM at 1 M LiCl, and 36 mM at 10 M LiCl.

Calcium Binding Experiments. Calcium binding was measured on the deuteriated POPS-containing samples used for the NMR experiments, which were prepared with $CaCl_2$ buffer solutions containing appropriate amounts of $^{45}CaCl_2$, such that their activities (A_0) were about 7000 cpm/μL. After the centrifugation step, the amount of radioactivity (A_f) was measured in the supernatant, and the free $CaCl_2$ concentration, $[Ca]_f$, was calculated as the total $CaCl_2$ concentration, $[Ca]_0$, multiplied by A_f/A_0. The bound fraction, $[Ca]_b$, was then obtained by subtracting $[Ca]_f$ from $[Ca]_0$. The radioactivities were counted with a Packard-2000Ca, on aliquots ranging from 10 to 50 μL, giving experimental values ranging between 20000 and 70000 (±100–200) cpm.

NMR Experiments. ^2H NMR experiments were done at 46 MHz on a homemade NMR spectrometer (Davis, 1979; Sternin, 1985). Spectra were acquired with a dwell time of 2 μs (POPS) or 5 μs (POPC) with 4096 data points and a repetition time of 150 ms. A quadrupolar echo pulse sequence (Davis et al., 1976) was employed with a pulse length of 4 μs and a pulse separation (τ) of 60 μs. The free induction decay was shifted by some fraction of the dwell time to ensure that its effective starting time for the Fourier transform corresponded to the top of the quadrupolar echo. Oriented ^2H NMR spectra were obtained by the numerical DePakeing procedure described by Sternin et al. (1983).

Results

Binding Studies. The binding data of Ca^{2+} obtained with POPC and POPC/POPS 5:1 liposomes are displayed in Figure 1 with a plot of the amount of membrane-bound Ca^{2+} versus the free amount of $CaCl_2$ present in the membrane suspension, both expressed in moles of Ca^{2+} per total lipid. Calcium binding is observed for both POPC and POPC/POPS 5:1 membranes. The POPC binding data are similar to those reported in previous Ca^{2+} binding studies showing a weak binding of Ca^{2+} to zwitterionic POPC (Lis et al., 1981; Macdonald & Seelig, 1987a). Incorporation of POPS in POPC leads to stronger calcium binding to the lipid bilayers. The curves represented on Figure 1 show that incorporation of 16.6% PS in the PC membranes leads to an approximate 3-fold increase of Ca^{2+} binding. It should be emphasized that the membrane-bound Ca^{2+} determined with this technique actually refers to all the Ca^{2+} ions accumulated at the membrane/solution interface; i.e., it contains both the ions adsorbed at the level of the lipid headgroups and the solvated ions located in the direct proximity of the membrane surface, which

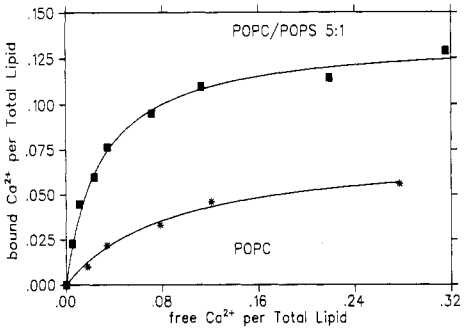

FIGURE 1: Binding of Ca^{2+} to POPC (*) and POPC/POPS 5:1 (M/M) (■) as a function of the amount of Ca^{2+} present in the lipid dispersion. The units are expressed as Ca^{2+} per total lipid. The total lipid concentration was 90 mM.

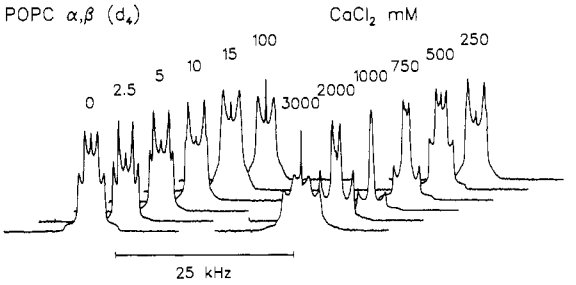

FIGURE 2: ^2H NMR spectra at 46 MHz of POPC α-CD_2 and POPC β-CD_2 recorded from POPC/POPS 5:1 (M/M) bilayers, with various concentrations of $CaCl_2$ at pH 7.5. Measuring temperature was 25 °C.

act simply as counterions of the negative lipid membrane.

Effect of Ca^{2+} on POPC Headgroups. Figure 2 displays ^2H NMR spectra (46 MHz) at 25 °C of POPC/POPS 5:1 membranes prepared with headgroup-deuteriated POPC and various amounts of $CaCl_2$. All spectra are typical of liquid-crystalline bilayers. At $CaCl_2$ concentrations above 3 M, line shapes become broader (data not shown), suggesting the formation of a gel phase. This is confirmed by the observation that, at 4 M $CaCl_2$, heating the sample up to 40 °C restores a sharp liquid-crystalline-phase spectrum. Each spectrum shows two quadrupolar splittings, associated with the α- and β-CD_2 group of the choline. Previous experiments (Scherer & Seelig, 1987) carried out with membranes containing PS and specifically headgroup-deuteriated POPC, in the absence of $CaCl_2$, have shown that the larger and the smaller quadrupolar splitting are respectively attributed to the α-CD_2 and β-CD_2 methylene of the choline moiety. Figure 2 shows that the addition of increasing amounts of $CaCl_2$ induces a decrease of the choline α-CD_2 quadrupolar splitting and an increase of the β-CD_2 splitting. The two splittings cross around 100 mM $CaCl_2$ and become resolved again after addition of higher concentrations of $CaCl_2$ up to 3 M. Quadrupolar splittings of the Depaked POPC spectra are plotted in Figure 3 as a function of the $CaCl_2$ added. For both the α and β splittings, the curve can be divided into two distinct regions. At low $CaCl_2$ concentrations (<0.1 mM; see insert), the quadrupolar splitting changes are steeper than at higher concentrations (0.1–3 M) where the variations are smoother and almost linear. The α and β quadrupolar splittings could not be reliably separated between 15 and 100 mM due to overlapping of the Depaked NMR lines. Our data obtained with POPC α,β (d_4)/POPS 5:1 membranes are qualitatively very similar to the results reported by Seelig's group in their studies of the interaction of Ca^{2+} with lipid membranes containing headgroup-deuteriated POPC, particularly those obtained with POPC/POPG 3:1 (Macdonald & Seelig, 1987a). From such

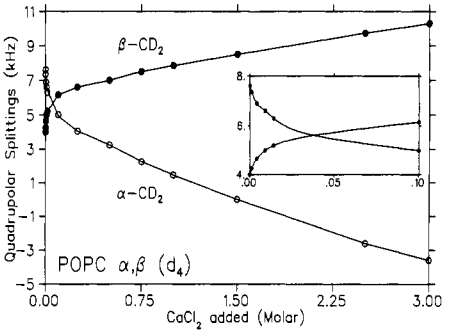

FIGURE 3: Calcium binding to POPC/POPS 5:1 (M/M) membranes as monitored by variations of the POPC headgroup quadrupolar splittings. The figure represents the variation of the POPC α (○) and β (●) quadrupolar splittings as a function of the calcium added. The insert shows an expanded plot of the low $CaCl_2$ concentration region. The solid curve in the insert is an example of data interpolation carried out in this concentration range.

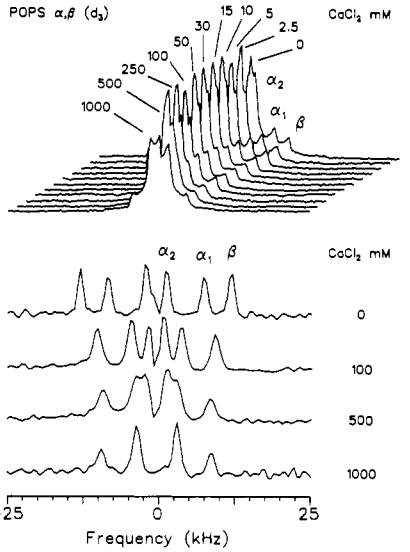

FIGURE 4: ^2H NMR spectra at 46 MHz of POPS α-CD_2 and POPS β-CD recorded from POPC/POPS 5:1 (M/M) bilayers, with various concentrations of $CaCl_2$ at pH 7.5. Measuring temperature was 25 °C. Selected Depaked spectra are shown on the bottom of the figure.

data, these authors have developed a quantitative analysis of Ca^{2+} binding based on a combination of the Gouy-Chapman theory with a simple Langmuir adsorption model. The application of this model to our POPC/POPS data will be discussed in the following section.

Effect of Ca^{2+} on POPS Headgroups. The ^2H NMR spectra represented on the top of Figure 4 were obtained with membranes identical with those described above, with the exception that the deuterons are now on the POPS headgroup. Selected Depaked spectra are also represented on the bottom of Figure 4. These spectra show three distinct quadrupolar splittings, two of which, $\Delta\nu_1$ and $\Delta\nu_2$, are associated with the two deuterons of the α-CD_2 methylene, denoted by α_1 and α_2, respectively, and a third one, $\Delta\nu_3$, with the β-CD of the serine moiety. The different values of $\Delta\nu_1$ and $\Delta\nu_2$ are almost certainly due to the inequivalence of the two α-CD_2 deuterons (Browning & Seelig, 1980). Strong evidence for the validity of this interpretation is provided by the observation that the ratio of the areas measured under the Depaked NMR lines of the two α deuterons is always close to 1 for all the data obtained up to now with headgroup-deuteriated PS (see Figure 4).

Incorporation of increasing amounts of $CaCl_2$ in the lipid dispersion leads to a gradual continuous decrease of $\Delta\nu_1$ and $\Delta\nu_3$ whereas $\Delta\nu_2$ appears to be less affected. Liquid-crys-

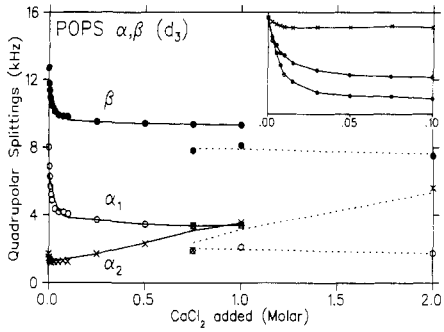

FIGURE 5: Calcium binding on POPC/POPS 5:1 (M/M) membranes as monitored by variations of the POPS headgroup quadrupolar splittings. The figure represents the variation of the POPS α_1 (○), α_2 (×), and β (●) quadrupolar splittings as a function of the calcium added. The solid and dotted lines denote experiments carried out respectively at 25 and 40 °C. The insert shows an expanded plot of the low $CaCl_2$ concentration region, in which *relative* variations of the quadrupolar splittings are plotted for a better display of the data.

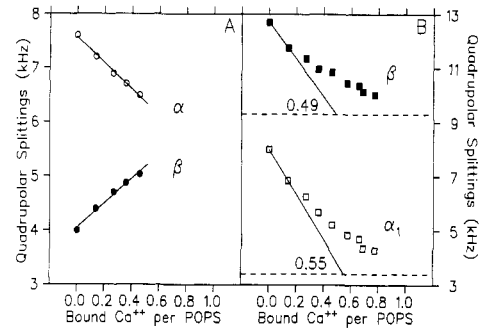

FIGURE 6: Variation of the POPC (panel A) and POPS (panel B) headgroup quadrupolar splittings as a function of the amount of Ca^{2+} bound to POPC/POPS 5:1 (M/M) membranes, expressed as moles of calcium per mole of POPS. (Panel A) POPC α (○) and β (●) quadrupolar splittings. The solid lines were obtained by linear regression analysis of the data points, giving the following correlations: $\Delta\nu_\alpha = -86.5X_{b(Ca^{2+})} + 7.56$ and $\Delta\nu_\beta = +81.6X_{b(Ca^{2+})} + 4.04$, with $X_{b(Ca^{2+})}$ being the moles of bound Ca^{2+} per mole of POPS. With $X_{b(Ca^{2+})}$ expressed in moles of bound Ca^{2+} per *total lipid*, the slopes are respectively −14.4 and 13.6 for $\Delta\nu_\alpha$ and $\Delta\nu_\beta$. (Panel B) POPS α (□) and β (■) quadrupolar splittings. The plateau values of the α and β POPS splittings are represented by the horizontal discontinuous lines at respectively 3.3 and 9.3 kHz. The solid lines were obtained by linear regression analysis of the first data points of each curve. The intercepts of these lines with the abscissa at their associated plateau values are expressed in bound Ca^{2+} per POPS. The membrane-bound Ca^{2+} was determined by $^{45}CaCl_2$ binding studies, performed on the headgroup-deuteriated POPS-containing samples used to record the NMR data represented in panel B. The corresponding POPC quadrupolar splittings (panel A) were extrapolated from the curves of Figure 3.

talline-phase spectra were obtained at 25 °C up to 1 M. Higher concentrations (2 M) of $CaCl_2$ lead to a severe broadening of the NMR line (data not shown). Such broadening can be eliminated if the temperature is increased, indicating that this effect is likely to be due to a liquid-crystalline to gel phase transition. It should be noted that, for the POPC headgroups, in the same conditions, this effect was observed only above 3 M $CaCl_2$, suggesting that a certain degree of POPS phase separation occurs above 1 M $CaCl_2$.

All the NMR spectra recorded with $CaCl_2$ concentrations where the POPS is in the liquid-crystalline phase display only one component, showing that the rate of exchange of lipid between the perturbed and the unperturbed states must be fast on the ^2H NMR time scale (10^{-5}–10^{-6} s). The POPS NMR data obtained in POPC/POPS 5:1 membranes contrast with the spectra recorded in pure POPS dispersions, for which a second large component ($\Delta\nu \approx 120$ kHz) was detected in the presence of calcium (M. Roux, unpublished results). This component is attributed to dehydrated $POPS(Ca)_2$ complexes known to occur under such conditions (Portis et al., 1979; Hope & Cullis, 1980; Feigenson, 1986). Indeed, the detection of this broad NMR component is in the present case strongly hampered by the loss of signal due to the 5-fold dilution of the PS molecules in PC, and the observation of a single liquid-crystalline component on the NMR spectrum does not preclude that a certain fraction of the PS molecules could be involved in a complex similar to that observed with pure POPS. An upper limit of this fraction can, however, be determined by the ratio of the spectral areas measured in the absence and presence of calcium (Tilcock et al., 1984). The ratio of the liquid-crystalline component areas measured at 0 and 1 M $CaCl_2$ was calculated here at 25 °C and found to be 1 ± 0.05, demonstrating that a large majority of the POPS molecules were in the liquid-crystalline state at this temperature in the presence of 1 M $CaCl_2$.

As shown on Figure 4, Depakeing of the NMR data allows a more accurate measure of the POPS quadrupolar splittings (compare original and Depaked spectra at 0.5 M $CaCl_2$), thus providing a better appreciation of the effect induced by the binding of the Ca^{2+} ions to the lipid bilayers. These effects are represented on Figure 5. As observed with the POPC NMR data, the calcium binding isotherms provided by the α_1 and β quadrupolar splittings of the POPS headgroup show that large variations occur at low $CaCl_2$ concentrations. A striking difference is that in the case of the POPS quadrupolar splittings, the perturbations appear to be quickly *saturable* since a plateau effect is clearly detected for $CaCl_2$ concentrations above 0.1 M. The minimum values measured at 25 °C and 1 M $CaCl_2$ are respectively 3.3 and 9.3 kHz for the α_1 and β splittings. Increasing the temperature to 40 °C allowed us to record NMR data at 2 M $CaCl_2$. Aside from the effect of increasing the temperature which gave rise to a decrease of the POPS quadrupolar splittings, it can be seen that a plateau is still observed at high levels of $CaCl_2$ at, respectively, 1.6 and 7.5 kHz for the α_1 and β splittings. In the absence of salt, the α_1 and β splittings showed, respectively, a decrease of 2.0 and 1.5 kHz upon heating from 25 to 40 °C (data not shown), which parallels the difference between the plateau values measured at 25 and 40 °C (respectively 1.8 and 1.8 kHz). The behavior of the α_2 splitting parallels those of the other PS splittings at low $CaCl_2$ concentrations (see Figure 5, insert). However, at higher salt concentrations, an opposite effect is observed, characterized by a large *increase* of the α_2 splitting values in contrast to the saturation effect observed with the α_1 and β doublets.

The data of Figures 3 and 5 are expressed as a function of the total $CaCl_2$ concentration. In Figure 6, POPC (panel A) and POPS (panel B) data are plotted versus the amount of membrane-bound Ca^{2+}. The amount of bound calcium was determined up to 40 mM $CaCl_2$ (0.78 Ca^{2+} per POPS) on the deuteriated POPS-containing samples used to record the NMR data of Figures 4 and 5. The corresponding POPC quadrupolar splittings were extrapolated from the curves of Figure 3. The variations of the POPS quadrupolar splittings (Figure 6B) are clearly not linear with the amount of membrane-bound Ca^{2+} determined in the $^{45}CaCl_2$ studies. This effect is more important at low Ca^{2+} binding. The intercepts, expressed as Ca^{2+} per POPS, of the solid lines drawn through the first data points of each curve with the abscissa at the corresponding plateau values of the quadrupolar splittings are 0.49 for the α_1 splitting and 0.55 for the β splitting. Due to the lack of reliable POPC data between 15 and 100 mM $CaCl_2$, we were not able to relate the Ca^{2+} binding to the POPC quadrupolar

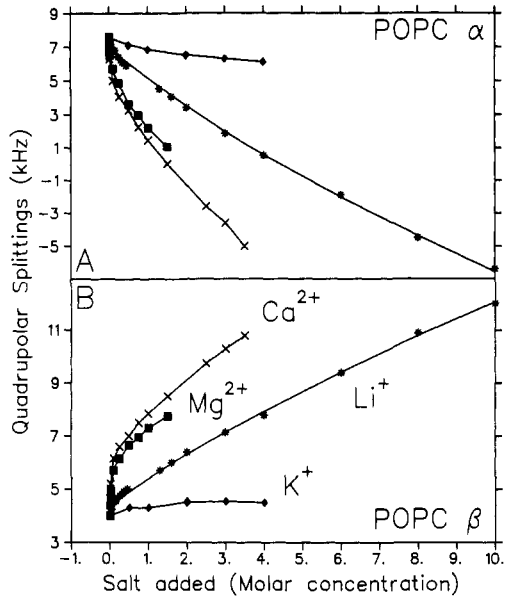

FIGURE 7: Calcium (×), magnesium (■), lithium (*), and potassium (♦) binding on POPC/POPS 5:1 (M/M) membranes as monitored by the variations of the POPC headgroup quadrupolar splittings. The figure represents the variation of the POPC α (panel A) and β (panel B) quadrupolar splittings as a function of the total salt added in molar concentration.

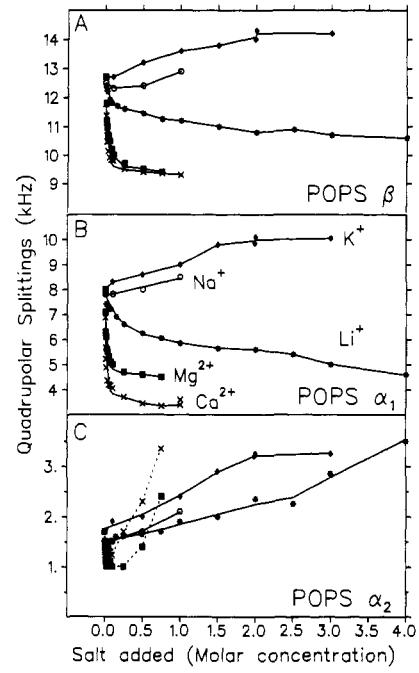

FIGURE 8: Calcium (×), magnesium (■), lithium (*), sodium (○), and potassium (♦) binding on POPC/POPS 5:1 (M/M) membranes as monitored by the variations of the POPS headgroup quadrupolar splittings. The figure represents the variation of the POPS β (panel A), α_1 (panel B), and α_2 (panel C) quadrupolar splittings as a function of the total salt added in molar concentration. The dashed lines of panel C were drawn for a better appreciation of the data. Note that all samples contained 100 mM NaCl, except when the NaCl dependence was under study (○).

splittings above 0.5 Ca^{2+} per POPS. Within the limits of this range, it can be said that both POPC quadrupolar splitting show a quasi-linear dependence with the concentration of membrane-bound Ca^{2+}. After conversion of the abscissa units to Ca^{2+} bound per total lipid, the values of the slopes measured on Figure 6A are, respectively, −14.4 and 13.6 for the α and β splittings. The slope measured with the α splitting is close to that reported in analogous ^2H NMR studies of Ca^{2+} binding to negative membranes containing headgroup-deuteriated POPC (Macdonald & Seelig, 1987a) (−16.7 for POPC/POPG 4:1).

Effect of K^+, Na^+, Li^+, and Mg^{2+} on POPC and POPS Headgroups. NMR experiments, similar to those described above with Ca^{2+}, were carried out with monovalent and divalent cations, Na^+, K^+, Li^+, and Mg^{2+}. All data were obtained with samples prepared in a buffer containing 100 mM NaCl, except for those describing the NaCl dependence. The results obtained with POPC and POPS headgroups are plotted, respectively, in Figures 7 and 8.

Figure 7 shows that the monovalent and divalent cations studied here have an effect qualitatively similar to that observed in the presence of Ca^{2+}, i.e., respectively a decrease and an increase of the α and β deuteron quadrupolar splittings of the choline headgroup, although the amplitude of the effect depends strongly on the nature of the cation considered. The divalent cations are more effective than the monovalent species, and the amplitudes of the variations are, in order of importance, $Ca^{2+} > Mg^{2+} > Li^+ > K^+$. For a concentration of 1 M salt added to the POPC/POPS 5:1 membranes, the size of the α splitting shows, respectively, a 81, 71, 34, and 10% decrease. The adsorption isotherm of Mg^{2+} is very similar to that of Ca^{2+} in the sense that (i) it shows a marked difference between a fast and a slow regime of the quadrupolar splitting changes at, respectively, low and high $MgCl_2$ concentrations and (ii) sharp liquid-crystalline phase spectra could only be observed up to 3 M salt, broad lines being observed at higher amounts of $MgCl_2$ (data not shown). In this regard, the case of Li^+ appears to be somewhat different to what is observed with divalent cations. The adsorption isotherm is very smooth over the whole concentration range, with no clearly marked changes in the slope of the curve, and sharp well-resolved deuterium powder patterns were observed up to very high salt concentrations (10 M LiCl). Thus, although the quadrupolar splittings are less sensitive to small amounts of Li^+ than to Ca^{2+} and Mg^{2+}, it is with this monovalent ion that the largest changes (α and β splittings of, respectively, −6.4 and 12 kHz) were detected. Although significant, the quadrupolar splitting changes detected with K^+ are much smaller than the variations observed with the other cations investigated here. Due to the lower water solubility of KCl compared to LiCl, the concentration range studied for this salt could not be extended beyond 4 M. The KCl and LiCl data were mainly obtained by raising the salt concentrations directly in the lipid pellet, followed by freezing and thawing of the membranes. We have found that this procedure could lead to small but systematic deviations of quadrupolar splittings (≈0.3 kHz) as compared to those recorded from samples dispersed in a buffer already containing the desired salt concentration. These deviations resulted in an underestimate of the β splittings, and an overestimate of the α splittings. This problem was avoided in the case of the $CaCl_2$ and $MgCl_2$ data by using a larger number of samples. The bound fractions of the monovalent cations and Mg^{2+} were not measured, and the data shown on Figure 7 are expressed as a function of the *total* salt concentrations. It is then very likely that the differences observed here are at least partly related to the various binding affinities of these cations for the lipid membranes.

As for the choline headgroup, the perturbations induced by Mg^{2+} and Li^+ on the α_1 (Figure 8B) and β (Figure 8A) quadrupolar splittings of the serine headgroups are qualitatively similar to those observed in the presence of Ca^{2+}, and the relative potencies of these cations also follow the order $Ca^{2+} > Mg^{2+} > Li^+$. The curves describing the Mg^{2+} adsorption

to the POPC/POPS 5:1 membranes show a plateau effect, after a sharp decrease of the two POPS splittings at low $MgCl_2$ concentrations, although the errors on the limiting values here are large due to the broadening of the NMR lines. A puzzling feature is that this broadening of the POPS NMR lines observed at high $MgCl_2$ concentrations is observed neither with the complementary POPC data nor with the related POPS data obtained with $CaCl_2$. We do not have an explanation for this phenomenon yet. The Li^+ adsorption isotherms are smoother than those observed with the divalent cations, the plateau being consequently less well-defined with these ions. The variations measured for the α_2 splitting (Figure 8C) in the presence of $MgCl_2$ are qualitatively similar to those observed with $CaCl_2$, namely, a steep decrease at low salt levels (<50 mM) and an increase at higher salt contents (>100 mM). The same remarks hold also for the LiCl data, with the exception that the variations are again much smoother. Although liquid-crystalline phase data could be recorded for a higher range of LiCl concentrations (up to 1 M for $MgCl_2$ and $CaCl_2$ and 4 M for LiCl), the maximum amplitudes of the effects measured for the three POPS quadrupolar splittings with this salt did not exceed those obtained with the divalent cations. The fact that gel phase-like spectra were obtained at lower salt concentrations for POPS than for POPC indicated that POPS phase separation also occurs in the presence of $MgCl_2$ and LiCl.

The effects of K^+ and Na^+ on the three POPS headgroup quadrupolar splittings appear to be quite special considering that they are qualitatively *opposite* to those observed with Li^+ and the divalent cations; i.e., the values of the β and both α splittings are *increased* in the presence of KCl or NaCl. The variations are smooth over the whole range of concentrations studied. The quadrupolar splittings measured in the absence of NaCl, respectively 7.8, 1.5, and 12.5 kHz for the α_1, α_2, and β quadrupolar splittings, are not very different from those measured in the presence of 100 mM NaCl (respectively 8.0, 1.7, and 12.7 kHz). Although the effects are more important for LiCl than for KCl at low salt concentrations for the POPS α_1 and β splittings, the *absolute* variations observed with the two monovalent salts at 2 M are comparable. For the same concentration, the corresponding variations of the POPC headgroup quadrupolar splitting are 4 times larger with LiCl than with KCl (Figure 7).

At high salt levels, it can be seen from Figure 8C that the increase of the α_2 splitting is about 2–3 times steeper for the divalent cations than for the monovalent cations, the respective slopes of the latter being otherwise similar. Figure 8C also shows that at low salt levels, the α_2 splitting is not decreased upon addition of KCl, whereas it shows an initial small decrease at low levels of LiCl. The same effect was reported in similar studies of Li^+ interactions with DMPC/DMPS 3:1 (M/M) membranes (Roux & Neumann, 1986).

POPS Interactions with $K_2GL_{20}K_2A$. ^2H NMR data describing the interactions of headgroup-deuteriated DMPC and DMPS with the cationic integral peptide $K_2GL_{20}K_2A$ have been shown to reflect charge-induced conformational changes of the headgroups (Roux et al., 1989) related to headgroup perturbations observed under similar conditions when metallic cations bind to the same membranes (Roux & Neumann, 1986). These experiments were partially reproduced in the present study (spectra not shown), with unsaturated POPC/POPS 5:1 membranes. As seen from Table I, the effect observed after incorporation of peptide $K_2GL_{20}K_2A$ is very similar to that previously reported in the saturated DMPC/DMPS 5:1 systems, in particular, an important decrease of the POPS α_1 and β quadrupolar splittings. A significant difference is that the POPS α_2 splitting is also decreased, unlike that of DMPS which has been shown to remain constant up to 0.3 mol of peptide per PS. However, the decrease is still much smaller than that of the α_1 splitting. Finally, we note that (1) the minimum values of the α_1 and β quadrupolar splittings reached after incorporation of 0.5 peptide per POPS are much lower than the plateau values measured in POPC/POPS 5:1 membranes at high $CaCl_2$ concentrations (Figure 5) and (2) the quadrupolar splittings measured after the approximate neutralization of the negative PS charges by 0.2 peptide per POPS are close to the plateau values detected in the presence of calcium.

Table I: Deuterium Quadrupolar Splittings (kHz) of Headgroup-Deuteriated POPS Obtained from Depaked Liquid-Crystalline Phase Spectra of POPC/POPS 5:1 (M/M) Membranes (25 °C) in the Presence of Various Amounts of Peptide $K_2GL_{20}K_2A^{5+}$

	mol of peptide/mol of POPS					
	0	0.1	0.2	0.3	0.4	0.5
POPS α_1	8.0	5.1	3.1	1.2	0	−1.00
POPS α_2	1.7	1.5	1.4	1.2	1.1	1.00
POPS β	12.7	10.7	9.6	8.2	7.1	6.20

Discussion

POPC Interactions with Ca^{2+}. The response of the PC headgroup to the interaction of Ca^{2+} ions with PS-containing membranes matches those observed by Macdonald and Seelig (1987a) under similar conditions in PG-containing membranes. The basis of this response lies in the concept that the choline headgroup acts as a "molecular electrometer" as delineated by Seelig et al. (1987), following the observation that the variations of the choline quadrupolar splittings were correlated with changes of the charge density at the membrane surface.

Hence, the choline α quadrupolar splitting was increased (decreased) after adsorption of negative (positive) charges at the membrane surface, whereas the β splitting changed in the opposite sense. Experimental data obtained with various charged molecules such as metallic cations, lipids, peptides, or anesthetics indicate that, qualitatively, these changes in the quadrupolar splittings are determined by the net charge of these compounds, irrespective of their chemical structure. This particular property of the PC polar headgroup has been used to monitor Ca^{2+} binding to PC-containing membranes over a wide range of $CaCl_2$ concentrations (up to 4 M), by estimating the fraction of membrane-bound Ca^{2+} from the values of the quadrupolar splittings [see Macdonald and Seelig (1987a) and references cited therein]. These analyses were made following the observation that, at low $CaCl_2$ concentrations, there was a linear relationship between the quadrupolar splitting variations and the *amount* of membrane-bound Ca^{2+} measured by absorption spectroscopy, and by assuming that this correlation was still valid at higher salt levels.

The correlation of the Ca^{2+} binding studies, carried out at low levels of $CaCl_2$ (0–15 mM), with the ^2H NMR data (Figure 6A) shows a linear dependence of the quadrupolar splittings of the POPC headgroup up to 0.5 Ca^{2+} per POPS. Attempts to relate the POPC quadrupolar splittings to higher amounts of membrane-bound Ca^{2+} by interpolation of the data between 0 and 0.1 M $CaCl_2$ (see insert of Figure 3) suggest that a discontinuity occurs above 0.5 Ca^{2+} per POPS, in the slope of the quadrupolar splitting versus the number of bound ions. This could not be unambiguously established due the small number of experimental data. However, strong evidence of a discontinuity of the slope for bound Ca^{2+} is provided by

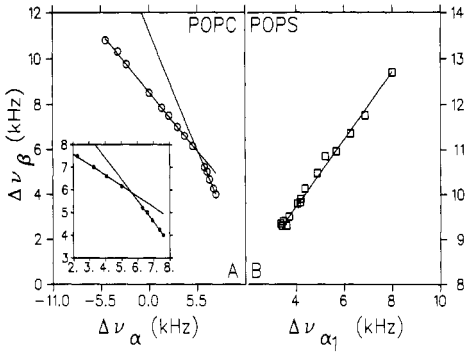

FIGURE 9: α,β plots obtained by plotting the β quadrupolar splitting as a function of the related α splitting, measured from ^2H NMR spectra of POPC/POPS 5:1 (M/M) membranes containing headgroup-deuteriated POPC (○) or headgroup-deuteriated POPS (□) in the presence of $CaCl_2$. The straight lines were calculated by linear regression analysis of the data points and are, in kilohertz, $\Delta\nu_\beta = -0.94\Delta\nu_\alpha + 11.16$ and $\Delta\nu_\beta = -0.47\Delta\nu_\alpha + 8.52$ for POPC (panel A) and $\Delta\nu_\beta = +0.72\Delta\nu_{\alpha_1} + 6.90$ for POPS (panel B).

the plot of the choline β quadrupolar splitting as a function of the α splitting (α,β plot) which allows a qualitative analysis of the NMR results obtained with the metallic cations, for which no determination of the concentration of bound cations was available. Such a representation (Figure 9A) of the Ca^{2+} data shows that a linear relationship is obtained with a discontinuity in the slope, which is −0.94 at low $CaCl_2$ concentrations and −0.47 at higher levels of salt.[2] On the α,β plot of Figure 9A, the change in the slope occurs when the α and β splittings are, respectively, 5.6 and 5.9 kHz. This discontinuity in slope of the α,β plot implies unequivocally that the slope of the Ca^{2+} dependence of at least one POPC quadrupolar splitting must be modified, although no indication is given of the exact value of each of these slopes above the discontinuity. Still, this question can be addressed in more detail through the analysis of previous ^2H NMR data reported by Seelig's group. The discontinuity observed with the divalent cation binding data, between negative and positive membranes, is an outcome of a recurring feature of the "molecular electrometer" properties of the choline headgroup introduced by Seelig et al. (1987). Such discontinuities in α,β plots of NMR data of headgroup-deuteriated PC-containing membranes have been observed in the presence of various types of charged molecules (Seelig et al., 1987; Scherer & Seelig, 1989), yielding a slope of −0.55 ± 0.15 for positive membranes and −1.0 ± 0.15 for negative membranes. Studies carried out with positive and negative amphiphiles (Scherer & Seelig, 1989), and hydrophobic anions and cations (Seelig et al., 1987), for which the NMR data could be directly related to the exact amount of bound charges, have demonstrated that the relative changes (slopes) of the POPC α-CD_2 quadrupolar splittings were larger with the positively charged molecules than for their negative analogues. These results have led the authors to propose that modifications of the membrane surface charge density were associated with two conformational changes of the phosphocholine headgroup, one being observed with negatively charged membranes, while the other is encountered with positively charged bilayers (Scherer & Seelig, 1989). Thus, these remarks suggest that the discontinuity observed for the α,β plot of the POPC data obtained with $CaCl_2$ could be associated with larger variations of the α splitting after neutralization of the negative PS-containing bilayers. Indeed, the situation encountered with Ca^{2+} binding to negatively charged membranes is special in the sense that the lipid composition remains the same, while the sign of the membrane charge density occurs through the neutralization of the anionic phospholipids by metallic cations. Still, the *absolute* values of the slopes measured here for each POPC quadrupolar splitting upon calcium binding to *negative* POPC-containing membranes (Figure 6A) are similar to those measured after incorporation of negative amphiphiles in pure POPC (Scherer & Seelig, 1987, 1989).

POPS Interactions with Ca^{2+}. PS headgroups have been shown to be sensitive to the charge distribution at the membrane surface, following the interaction of the bilayers with cations (Roux & Newmann, 1986) or charged peptides and proteins (Roux et al., 1989; Bitbol et al., 1989; Dempsey et al., 1989). Thus, it is not surprising that the adsorption of Ca^{2+} to POPC/POPS 5:1 membranes induces large variations of the serine headgroup quadrupolar splittings. The key observation here is that these variations show saturation behavior as can be seen very clearly from Figure 5. In this respect, the serine ^2H NMR data differ markedly from those of choline for which such saturation behavior was not detected upon adsorption of $CaCl_2$. In the absence of $CaCl_2$, the incorporation of 0.5 mol of peptide $K_2GL_{20}K_2A$ per mole of POPS leads to values of the α_1 and β quadrupolar splittings as low as, respectively, −1 and 6.1 kHz (Table I). Moreover, with Ca^{2+} binding to POPC/POPS/$K_2GL_{20}K_2A$ 5:1:0.2 (M/M/M) (Roux and Bloom, unpublished data), the plateau values obtained for the POPS splittings above 0.1 M salt were significantly lower (2.4 and 8.3 kHz) than those reported here (3.6 and 9.3 kHz) without peptide. Thus, charge-induced variations of the POPS quadrupolar splittings can be far greater than the plateau values measured in the $CaCl_2$ experiments. The fact that the POPS splittings do not exceed these plateau values beyond a certain amount of $CaCl_2$ should consequently not be associated with a final "locked" state of the molecular perturbation of the serine headgroup. It rather indicates that the binding of additional Ca^{2+}, suggested by the PC headgroup NMR data, must occur at a different site. This particular feature of the PS headgroup brings us to the straightforward conclusion that at least two modes of Ca^{2+} binding must be considered. The first one would be associated with the large variations of the serine headgroup α_1 and β quadrupolar splittings observed upon binding of Ca^{2+} at low $CaCl_2$ contents and the second one only with perturbations of the α_2 splitting at higher salt levels, where the α_1 and β quadrupolar splittings are not modified anymore. As a first interpretation, we could consider two classes of *laterally* segregated Ca^{2+} binding sites at the membrane surface, one site associated with PS headgroups and the other composed exclusively of PC headgroups. To be compatible with the observation that the Ca^{2+} ions are in fast exchange between lipid headgroups, such an interpretation would assume a certain degree of lateral separation of the PS molecules. A second explanation involves a *transverse* distribution of the Ca^{2+} binding sites; i.e., different sites are differentiated by the depth at which the Ca^{2+} ions are bound. In any case, the interpretation should take into account that the lateral diffusion of the Ca^{2+} ions is rapid on the NMR time scale, the ions being in fast exchange among the ensemble of lipid headgroups.

Figure 6B shows that the POPS quadrupolar splittings and the *total* amount of membrane-bound Ca^{2+} determined by

[2] The α,β plot obtained with Mg^{2+} ^2H NMR data also shows a similar discontinuity, leading to a steeper slope (0.80) at low salt concentrations and a lower slope (0.44) at higher $MgCl_2$ levels. This discontinuity is less clearly defined on the α,β plots obtained with LiCl and KCl data. We believe this latter finding is due to deviations of the data measured in the LiCl- and KCl-containing samples as mentioned previously (see Results).

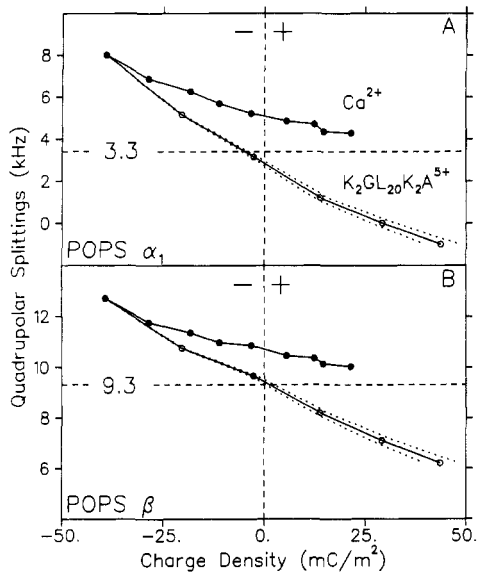

FIGURE 10: Comparative analysis of the perturbations of POPS headgroup quadrupolar splittings induced by Ca^{2+} ion (●) and peptide $K_2GL_{20}K_2A$ (○) binding to POPC/POPS 5:1 (M/M) membranes. (Panel A) POPS α_1 splitting. (Panel B) POPS β splitting. The quadrupolar splittings (kilohertz) are plotted as a function of the *net* charge density (millicoulombs per square meter) at the membrane surface which is the sum of the negative charge density associated with the PS molecules with the positive charge density generated by the calcium (or peptide $K_2GL_{20}K_2A$ charges). The peptide curves were obtained by assuming a cross-sectional area of the peptide of 150 Å^2 (solid curve) ± 50 Å^2 (dotted curves). The vertical line at zero denotes the separation between negatively and positively charged membranes. The horizontal dashed lines indicate the values of the plateau reached by the POPS quadrupolar splittings in excess of $CaCl_2$.

$^{45}CaCl_2$ binding studies do not show a simple linear correlation. Previous NMR data describing the interaction of cationic peptides (Roux et al., 1989; Dempsey et al., 1989) with similar membrane systems (DMPC/DMPS 5:1) show that there is in fact a linear variation of the corresponding serine headgroup quadrupolar splittings with the variation in the membrane charge density associated with these peptides. These experiments were repeated in the present study with the integral peptide $K_2GL_{20}K_2A$ and the unsaturated POPC/POPS 5:1 membrane systems (Table I). The results are plotted in Figure 10, together with the calcium binding data. To allow a direct comparison of the calcium and peptide data, the abscissa is normalized in total charge density, σ_{total}, resulting from the incorporation of the cation X (peptide or calcium ion) in the negatively charged PS-containing membranes:

$$\sigma_{total} = \sigma_{PS} + \sigma_X \quad (1)$$

with (Seelig et al., 1988)

$$\sigma_{PS} = \frac{e_0 z_{PS}[PS]}{A_L + A_{PS}[PS]} \text{ and } \sigma_X = \frac{e_0 z_X X_b}{A_L + A_X X_b} \quad (2)$$

where z_X and z_{PS} are respectively the net charge of the membrane-bound species X and of POPS, X_b and [PS] are the molar fractions of these two components (in mole per mole of total lipid), and e_0 is the charge of the electron. A_L and A_X are respectively the cross-sectional areas of a lipid molecule and of the species X. We used the values $A_L = A_{PS} = 68$ Å^2 (Altenbach & Seelig, 1984), $A_{Ca^{2+}} = 0$, and $A_{peptide} = 150 \pm 50$ Å^2. The ±50 Å^2 uncertainty for $A_{peptide}$ has been estimated in an approximate manner from a molecular model and is represented on Figure 10 by the dotted curves drawn on each side of the experimental peptide data. Figure 10 confirms that the variation of the PS headgroup quadrupolar splittings with the charge density associated with the incorporation of peptide $K_2GL_{20}K_2A$ is quasi-linear. The curves obtained with Ca^{2+} binding indicate that the amplitudes of the quadrupolar splitting changes are almost equivalent to that induced by the peptide $K_2GL_{20}K_2A$ for the very first data points but are gradually attenuated upon additional Ca^{2+} binding. Thus, the Ca^{2+} charges are nearly as effective in perturbing the PS headgroup as those of the amphiphilic peptide $K_2GL_{20}K_2A$ in the *early* stage of binding, but become less and less effective as Ca^{2+} binding increases. This phenomenon can be explained by competition between two membrane Ca^{2+} sites, assuming that a growing fraction of the total bound Ca^{2+} starts to occupy a second membrane site before the complete saturation of the first site, i.e., before the POPS α_1 and β splittings reach their plateau values. Strictly speaking, our model is that of a primary binding site for Ca^{2+} and a secondary site which involves all other binding sites; i.e., it could correspond to a continuous distribution of charge along an axis transverse to the membrane surface. Indeed, this picture appears consistent with the experimental differences observed on Figure 10 between the $K_2GL_{20}K_2A$ and Ca^{2+} data, if we consider that the charges of the integral peptide $K_2GL_{20}K_2A$ are anchored in the lipid bilayer, whereas the Ca^{2+} ions are in a highly dynamic equilibrium between bound and free species, leading to a spreading of the transverse distribution function of the Ca^{2+} charges into the bulk solution along the normal to the bilayer surface. The peptide curves of Figure 10 intersect the Ca^{2+} plateau values (*horizontal dotted lines*) close to the point where the net charge is zero (*vertical dotted lines*), corresponding to the neutralization of the negative PS-containing bilayers by the cationic lysine residues of the integral peptide. This indicates that the final state of the POPS headgroups after saturation of the first site is *qualitatively* similar to that obtained when the negative net charge of the phosphoserine moiety is neutralized by one net positive charge provided by the amphiphilic peptide. The latter would support a 0.5 to 1 stoichiometry of Ca^{2+} to POPS at the first site, for which one Ca^{2+} charge exactly counteracts one POPS charge. A similar conclusion can actually be drawn from Figure 6B, which shows that for both the α_1 and β splittings the straight lines drawn through their first data points at low Ca^{2+} binding intersect their respective plateau values at respectively 0.55 and 0.49 Ca^{2+} bound per POPS.

Table II: Slopes of α,β Plots Obtained with POPC/POPS 5:1 (M/M) Membranes (25 °C, pH 7.5) in the Presence of Various Mono- and Divalent Cations[a]

	Ca^{2+}	Mg^{2+}	Li^+	Na^+	K^+	$K_2GL_{20}K_2A^{5+}$
POPS	0.72	0.90	0.60	0.73	0.74	0.72

[a] The slopes were calculated with linear least-squares fit analysis, from α,β plots of the Data displayed on Figure 8 (POPS). The α,β plot obtained with $CaCl_2$ data is represented on Figure 9.

Additional insight into the nature of the metallic cations binding to the PS-associated sites can be obtained from the α,β plot of the POPS NMR data (Figure 9B). Like the choline NMR data, this plot shows a linear relationship although no significant change in slope is detected. The linearity of the PS α,β plot contrasts with the nonlinear dependence of each splitting taken independently, with the amount of membrane-bound Ca^{2+} determined in the $^{45}CaCl_2$ studies. This observation supports the interpretation that only one type of perturbation should be considered through the whole range of variations of the α_1 and β quadrupolar splittings of the PS headgroup and that the nonlinearity discussed above should rather be associated with various Ca^{2+} binding sites. Besides, it can actually be seen from Table II that the value of the slope measured from the Ca^{2+} data is equal to that obtained from

Table III: Comparative Analysis of ^2H NMR Data Obtained with POPC and POPS Headgroups in POPC/POPS 5:1 (M/M) in the Presence of Various Metallic Cations[a]

	C_{50} (mM)[b]		POPS $\delta[\Delta\nu_{(\alpha_1)}]$ (kHz)		POPS $\delta[\Delta\nu_{(\beta)}]$ (kHz)	
POPC:	α(6.4)	β(5.2)	α(6.4)	β(5.2)	α(6.4)	β(5.2)
$CaCl_2$	15	15	−3.1 (−39)	−3.1 (−39)	−2.2 (−17)	−2.2 (−17)
$MgCl_2$	39	50	−2.6 (−33)	−2.7 (−34)	−2.1 (−16)	−2.2 (−17)
LiCl	260	550	−1.4 (−17)	−1.8 (−22)	−1.1 (−9)	−1.3 (−10)
KCl	3000		+2.1 (+26)		+1.5 (+12)	

[a] C_{50} values are the salt concentrations (millimolar) for which the values of the α and β POPC quadrupolar splittings are respectively 6.4 and 5.2 kHz, and $\delta[\Delta\nu_{(\alpha_1)}]$ and $\delta[\Delta\nu_{(\beta)}]$ are the corresponding relative variations of the α_1 and β POPS quadrupolar splittings in kilohertz. The values in parentheses are expressed as a percentage of the initial value measured in the absence of salt. [b] The upper limit of the error on C_{50} is estimated at 30%. This error is due to the extrapolation of C_{50} from the curves of Figure 7.

the α,β plot of the peptide $K_2GL_{20}K_2A$ data (not shown), thus sustaining the idea that the serine headgroup conformational changes induced by these two different molecular species are qualitatively similar. The correlation depicted in Figures 6B and 10 of the amount of membrane-bound Ca^{2+} with the POPS quadrupolar splittings was carried out up to 0.78 Ca^{2+} per POPS, but can be extended to higher amounts of Ca^{2+} binding through examination of the *relative* changes of the POPC and POPS quadrupolar splittings, as represented in Figure 11. Only relative variations of the quadrupolar splittings are represented on Figure 11, so that the data recorded in the absence of calcium correspond here to 0. The vertical lines denote discrete values of membrane-bound Ca^{2+} expressed in equivalents of Ca^{2+} per mole of POPS.[3] The first value (0.5 Ca^{2+}/POPS) was determined experimentally with $^{45}CaCl_2$ binding studies, whereas the other ones were extrapolated from the POPC NMR data as described by Macdonald and Seelig (1987a). For the latter, each additional equivalent is represented by a dotted box, which accounts for the uncertainty associated with this extrapolation, as discussed in the previous section. Nevertheless, it can be seen that significant variations of the POPS quadrupolar splittings are observed up to 3 equiv of bound Ca^{2+} ($\approx$0.5 M total $CaCl_2$), above which no detectable variations of the α_1 and β splittings are monitored. The behavior of the α_2 quadrupolar splitting shows an interesting correlation with the binding of each equivalent of Ca^{2+}. This splitting displays a small decrease during the adsorption of the first equivalent of Ca^{2+}, remains roughly constant with a second equivalent, and is sharply increased by the binding of additional amounts of Ca^{2+}, beyond the limit where the α_1 and β splittings are no longer affected. Therefore, the PS headgroups are still affected by the Ca^{2+} binding to the second class of sites, although the molecular response monitored by NMR is very different from the one observed during Ca^{2+} binding to the first sites. Additionally, we note that the plots of Figure 11 provide clear evidence that the correlation between the Ca^{2+}-induced conformational changes of the choline and the serine headgroups does not follow a simple linear relationship, and confirm that the responses of these two headgroups are decoupled and differ according to the extent of Ca^{2+} binding. A similar plot, leading to identical conclusions, can be obtained by replacing the relative variations of the POPC β splitting on the abscissa by those of the α splitting (not shown).

The emerging picture thus suggests two-step binding to the POPC/POPS 5:1 membranes, correlated to the saturation of two different kind of sites. Ca^{2+} binding to the first sites at low $CaCl_2$ concentration is nearly saturated around 0.5 M $CaCl_2$. Calcium interaction with the second sites starts prior to saturation of the first sites and shows no indications of saturation up to 3 M $CaCl_2$. It must be emphasized that the binding sites described here for ions introduced via the electrolyte solution should be viewed as highly dynamic sites, rather than well-defined static chemical complexes such as that obtained upon dehydration of pure PS bilayers by Ca^{2+} (Portis, 1979; Feigenson, 1986). Each site should be defined on the basis of a statistical distribution function of the cation in the bilayer and requires a good theory for the charge distribution of the electrolyte near the membrane interface. We will return to this point in the final section of this paper in "theoretical considerations" arising from these results.

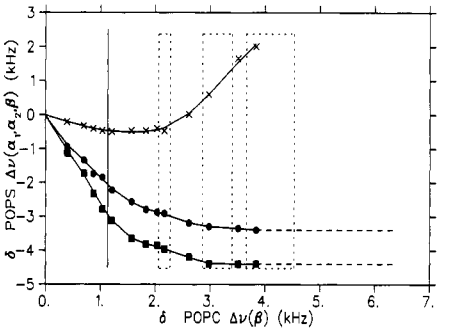

FIGURE 11: Plots of the relative variations (δ) of the POPS quadrupolar splittings [α_1 (■); α_2 (×); β (●)] versus the relative variations of the POPC β splitting. The relative variations of the quadrupolar splittings are such as $\delta_i = \Delta\nu_{i,0} - \Delta\nu_{i,x}$ where $\Delta\nu_{i,0}$ and $\Delta\nu_{i,x}$ are the values of the quadrupolar splitting i measured respectively in the absence or in the presence of the molar concentration x of salt. The POPC β and POPS α_2 splittings are represented by ($-\delta_i$). The solid vertical line denotes the quadrupolar splitting variations measured for 0.5 bound Ca^{2+} per POPS molecules, in correlation with the $^{45}CaCl_2$ binding studies. The dashed boxes indicate the range of presumed values (see text) of the POPC β quadrupolar splitting for which 1, 1.5, and 2 Ca^{2+} per POPS are bound to the membrane.

POPC and POPS Interactions with Mg^{2+}, Ca^{2+}, Li^+, K^+, and Na^+. The two-step binding proposed in the interpretation of calcium binding to POPC/POPS 5:1 membranes appears to be also appropriate to describe magnesium binding to the same membranes, since the NMR data obtained with these two divalent cations are comparable. LiCl, unlike NaCl and KCl, gives NMR data which can be qualitatively related to those obtained with the divalent cations, suggesting that two-step binding of Li^+ to POPC/POPS 5:1 membranes might also occur. Since the correlation between the NMR data and the extent of Mg^{2+}, Li^+, Na^+, and K^+ binding was not determined in the present study, the discussion of the NMR data obtained with these cations will be developed through a comparative analysis of these data with the Ca^{2+} results discussed in the previous sections. For this purpose, we use characteristic values of the POPC α quadrupolar splittings as a common reference indicator of the cation binding which would allow us to compare the ensemble of the NMR data obtained with all the cations investigated (Table III). These values are those measured after binding of 0.5 Ca^{2+} per POPS (6.4 and 5.2

[3] We define empirically 1 equiv of Ca^{2+} as 0.5 Ca^{2+}/POPS, the amount needed to neutralize the PS charges.

kHz for the α and β quadrupolar splittings, respectively), when the total $CaCl_2$ concentration is about 15 mM. These values are actually close to those measured in a buffered (pH 7.2) POPC bilayer in the absence of salts (Kuchinka & Seelig, 1989). This indicator will allow us to determine (1) C_{50}, the concentration of a given salt needed to obtain the same quantitative effect, extrapolated from the curves of Figure 7, and (2) the corresponding variations of the POPS α_1 and β quadrupolar splittings at this concentration, extrapolated from the curves of Figure 8. We note that the indices C_{50} should parallel the relative affinities of the metallic cations for POPC/POPS 5:1 membranes, if the correlation between the POPC headgroup perturbation, as viewed by ^2H NMR, and the amounts of bound cations determined in the $CaCl_2$ studies (Figure 6B) is the same for the other salts.

The relative differences observed between the effects induced by Ca^{2+}, Mg^{2+}, and Li^+, in POPC/POPS membranes, on the POPS NMR data conform to those obtained for the POPC headgroup and are both in the order $Ca^{2+} > Mg^{2+} > Li^+$. If we use the C_{50} index described above as an indicator of cation binding with the $MgCl_2$ data, we find that the PS charges should be neutralized in the same range of concentration found with $CaCl_2$, but at slightly higher values (Table III). This observation is in broad agreement with previous comparative binding studies of these two salts to the PS membrane compiled by Bentz et al. (1983). Binding of lithium to PS membranes and other monovalent cations is known to be at least 10 times weaker than divalent cation binding (Eisenberg et al., 1979; Cevc et al., 1984). This aspect of Li^+ binding is very likely the cause of the smooth Li^+ adsorption isotherms provided by the POPS NMR data. From Table III, it can be seen that the indicator values defined from the POPC Ca^{2+} binding data are obtained respectively at 0.26 M for the α and at 0.5 M for the β splitting. The lower limit of these values is at least an order of magnitude above the concentration of $CaCl_2$ required to bring down the corresponding POPC splitting to the same value, which is therefore in agreement with the studies cited above. The value of our C_{50} index extrapolated for K^+ should be of the order of that of Li^+, since the respective affinities of these two monovalent ions are similar (Eisenberg et al., 1979). The C_{50} value obtained for K^+ appears in this respect too large, and would imply that the affinity of Li^+ is about an order of magnitude higher than that of K^+. A possible explanation of this particular feature would be that the spatial distribution, relative to the choline headgroup, of the bound charges of K^+ ions is quite different from that of Li^+ ions.

The values of C_{50} listed in Table III can also be used to compare the POPS NMR data obtained with various salts. For instance, it can be seen from Table III that at 15 mM $CaCl_2$ the POPS α_1 and β quadrupolar splittings show a respective decrease of about 39% and 17%. Thus, for an equal change of the choline headgroup α splitting, it appears that the decrease sensed by the POPS splittings is about 2 times smaller for LiCl (respectively 20% and 10%) than for $CaCl_2$. In the case of $MgCl_2$, the difference is less important. These observations provide further support for the idea, developed in the two-step Ca^{2+} binding model described in the previous section, that the PC and PS headgroup responses to cation binding are independent, since at least *two* levels of perturbation of the serine quadrupolar splittings can be observed for *one* given change of the choline headgroup. Moreover, another distinct type of perturbation of the POPS headgroup is provided by the KCl (and NaCl) data, for which the variations of the serine quadrupolar splittings occur here in the *opposite* sense to those of the other cations. This particular effect of K^+ ions on the PS headgroup supports the idea that the distribution of this cation in POPC/POPS 5:1 membranes is different from that of the other cations.

Theoretical Considerations

Electrostatic Model for the Interaction of a Charge Distribution with Phospholipid Headgroups. As discussed in the preceding sections, a coherent analysis of the ^2H NMR data obtained upon metallic cations binding to POPC/POPS 5:1 membranes suggests that the observed charge-induced perturbations of the lipid headgroups depend not only on the concentrations of the bound charges but also on their spatial distributions in the headgroup region. Trying to correlate the headgroup conformational changes observed by ^2H NMR with the distribution function of the membrane-bound cations is in fact a logical extension of the simple electrostatic model developed in our previous paper (Roux et al., 1989), in which we have interpreted NMR data of headgroup-deuteriated lipids by considering a conformational change of the headgroups resulting from the interaction of their charges with the electric field associated with charges at or near the membrane surface. In the following, we first review briefly and extend slightly this electrostatic model and then relate it to our discussion of the NMR data obtained with metallic cations. Ultimately, however, the experimental results should be interpreted in terms of a more fundamental theory for ion charge distribution near membrane surfaces, such as that discussed briefly in the next section.

In the electrostatic model, the phospholipid molecule was represented as a cylinder of radius R and the membrane-bound charges were assumed to be located outside the cylinder. For a deuteron i of the polar headgroup, the change of the quadrupolar splitting $\Delta\nu_i$, $\delta(\Delta\nu_i)$, was expressed in terms of the rotation of the polar headgroup by a torque τ due to the interaction of the headgroup charge distribution with the surface charge density σ_k of charge species k modeled as a uniform thin layer of charge parallel to the membrane surface at a distance z_k from the center of the membrane [see Figure 9 of Roux et al. (1989)]. We summarize the results of this model calculation in terms of R,z_k, the effective vertical position z of the polar headgroup charge distribution, and a_{ik}, a factor involving other geometrical aspects of the polar headgroup. For $\delta(\Delta\nu_i)$ proportional to τ:

$$\delta(\Delta\nu_i) = \sum_k a_{ik}\sigma_k\left[\frac{z - z_k}{\sqrt{R^2 + (z - z_k)^2}}\right] \qquad (3)$$

In the original description of the model, the electric field due to σ_k, responsible for the torque leading to the change in quadrupolar splitting, was approximated to be that along the cylinder axis. This gives a coefficient a_{ik} independent of k so that eq 3 represents a small generalization of the original result, which allowed us to relate the sensitivity of $\Delta\nu_i$ to different charged moieties k in terms of their location z_k relative to the membrane surface (Roux et al., 1989). In order to take account of the fact that σ_k is expected to be distributed over a range of membrane depths about its average position z_k, we have to modify eq 3. For a *uniform* charge distribution between $z_k - W_k$ and $z_k + W_k$, it is easy to show that eq 3 becomes

$$\delta(\Delta\nu_i) = \sum_k \frac{a_{ik}\sigma_k}{2W_k}\left[\sqrt{R^2 + (z - z_k + W_k)^2} - \sqrt{R^2 + (z - z_k - W_k)^2}\right] \qquad (4)$$

For $(R^2 + W_k^2)^{1/2} \gg z - z_k$, eq 4 becomes

$$\delta(\Delta\nu_i) = \sum_k a_{ik}\sigma_k\left[\frac{z - z_k}{\sqrt{R^2 + W_k^2}}\right] \quad (5)$$

Therefore, the effective sensitivity of the quadrupolar splitting i with respect to a charge species k is proportional to $\sigma_k(z - z_k)$, in respect to *magnitude* and *sign*, for a thin distribution of membrane-associated charge, and decreases in *magnitude* in proportion to $(R^2 + W_k^2)^{1/2}$ as the width W_k of the charge distribution is increased. Although the calculation detailed here considers the simple case of a uniform charge distribution along the normal to the bilayer surface, it can be shown that the extension of this model to nonuniform distribution functions, e.g., Gaussian, or even a more general unsymmetric function leads to the same qualitative conclusion, namely, $\delta(\Delta\nu_i)$ is decreased when W_k is increased, although the relationships between these two quantities are in the latter cases more complex than eq 5.

In our original discussion of eq 3 (Roux et al., 1989), we concluded that the response of quadrupolar splittings of PS headgroup deuterons indicates that Li^+ ions bound to membranes of DMPC/DMPS 5:1 membranes are located below the lipid headgroups, at about the same depth as the lysine charges of the amphiphilic peptide $K_2GL_{20}K_2A$ in the same membranes ($z_k < z$). The observation that bound Na^+ ions give values of $\delta(\Delta\nu_i)$ close to zero led to the conclusion that they are located somewhat closer to the aqueous interface ($z_k \approx z$), while the opposite sign of $\delta(\Delta\nu_i)$ due to pentalysine was consistent with its binding sites being located on the outside of the membrane ($z_k > z$). In the light of eq 5, it is seen that the small values of $\delta(\Delta\nu_i)$ measured with Na^+ and pentalysine, as compared to those obtained with Li^+ ions and peptide $K_2GL_{20}K_2A$, could be partly due to larger widths W_k of their charge distributions.

^2H NMR data obtained with the peptide $K_2GL_{20}K_2A$ are very similar for both the saturated DMPC/DMPS and unsaturated POPC/POPS membrane systems, indicating, in line with our model, that the charges of the peptide $K_2GL_{20}K_2A$ are also located below the POPS headgroups. The fact that the effects induced by the first bound Ca^{2+} ions are similar to that of peptide $K_2GL_{20}K_2A$ indicates that the Ca^{2+} and peptide charges are located at approximately the same depth. The progressive attenuation depicted by Figure 10 of the charge-induced perturbation of the POPS headgroup observed with Ca^{2+} ion, as opposed to that of the integral peptide $K_2GL_{20}K_2A$, could then be related to a spreading out of the Ca^{2+} ion distribution along the bilayer normal toward the aqueous solution, and be viewed in eq 5 in terms of an increase of W_k, leading to reduced values of the quadrupolar splitting variations $\delta(\Delta\nu_i)$. Likewise, the gradual decrease in the magnitude of the POPS headgroup perturbation observed with other metallic cations in the order $Ca^{2+} > Mg^{2+} > Li^+$ (Table III) can be correlated to a decrease in the depth of the center of their distribution functions ($z_{Ca^{2+}} > z_{Mg^{2+}} > z_{Li^+}$), and/or broadening of the *width* of these functions ($W_{Li^+} > W_{Mg^{2+}} > W_{Ca^{2+}}$), observed if the cations are more spread out along the bilayer normal. The electrostatic model upholds implicitly the idea that one kind of perturbation of the serine headgroup should be associated with the binding of Ca^{2+}, Mg^{2+}, and Li^+ and that the experimental differences summarized in Table III lie in the amplitude rather than in the intrinsic nature of the perturbations. A perturbation of the PS headgroup common to the metallic cations is indeed supported by the observation that the slope values of their respective α,β plots (Table II) are reasonably close within the range 0.6–0.9. In particular, the slopes of the α,β plots obtained with the other monovalent cations K^+ and Na^+ fall within the range of values measured for the other cations, suggesting that the PS headgroup conformational change induced by these cations is related to that of the divalent cations. This result contrasts with the observation that the *sign* of the changes of each POPS splitting taken individually with K^+ and Na^+ is opposite to those observed with Li^+ and the divalent cations (Figure 8 and Table III). This particular feature can now be explained by assuming that, as for pentalysine in DMPC/DMPS membranes, these cations are located *above* the serine headgroup ($z_k > z$), toward the outside of the membrane, yielding a torque of the headgroup related to the one we associate with the effect of Li^+ and the divalent cations, but of an *opposite* sign. Thus, K^+ (Na^+ ions) would be less buried (and/or more scattered) in the bilayer than the other metallic cations and particularly Li^+.

Regarding PC headgroups, it seems that K^+ ions and pentalysine each induce surprisingly small perturbations of the choline quadrupolar splittings, too small to detect in the case of pentalysine (Roux et al., 1988), in contrast with all the other cationic molecules investigated (see above discussion of K^+ and Li^+ C_{50} indexes of Table III). Thus, location of positive charges on the outside of the headgroup region, as assumed for K^+ and pentalysine, would result in very small perturbations of the choline headgroup, in contrast with the larger effects observed with Li^+ ions and divalent cations, believed to be buried deeper in the bilayer.

Relationship with Fundamental Theories of Electric Fields near the Membrane Surface. Good theoretical models exist for treating the aqueous medium as a *continuum* in contact with smooth surfaces (McLaughlin, 1989). These models give useful information on the charge distributions far from the interface but break down at short distances, apparently because of the importance of the surface-induced structure of the aqueous medium extending out to distances of at least several molecular diameters (Ninham, 1989). Because of the sensitivity of ^2H NMR quadrupolar splittings to local, spatial charge distributions, as discussed above, it appears to us that experimental studies such as those reported here have much to contribute toward a solution to this important problem. Although there exists no theory that takes into account the role of surface-induced water structure near *rough* membrane surfaces, we are encouraged by the apparent connection between the systematics in the response of different ions as described in the simple, albeit incomplete, analysis of our data using the simple electrostatic model of the previous section and features described in a recently developed theoretical treatment of the influence of structured water near *smooth* surfaces on the spatial distribution of ions introduced as salt in the aqueous medium (Patey & Torrie, 1989; Torrie et al., 1989). It appears that when the structure of the solvent (water) molecules is taken into account, substantial deviations from the continuum (water) model are predicted in the form of large and quite narrow counterion peaks within a few angstroms of the smooth surface. The total counterion charge on these narrow peaks can be sufficient to neutralize the negative charges on the membrane, or even greater. Although explicit theoretical results have only been published for a small number of ions [see, e.g., Figures 6 and 7 of Torrie et al. (1989) for Na^+ and K^+ near a neutral and a negatively charged surface, respectively], it appears that the systematic variation of position and width of such peaks can well be compared with the systematic variations for Ca^{2+}, Mg^{2+}, Li^+, Na^+, and K^+ discussed for the

primary "binding site" in the preceding analysis (G. N. Patey, personal communication). What is needed now is a direct calculation of torques on the PC and PS headgroup as a function of surface charge and salt concentration, using the detailed ion charge distribution evaluated by Patey, Torrie, and their collaborators, or some equivalent fundamental theory of the distribution of ion charges near interfaces.

Conformation of the Choline and Serine Headgroups. It is generally agreed that the orientation of the choline segment is essentially parallel (within about 30°) to the membrane surface (Pearson & Pascher, 1979; Büldt et al., 1978) when the net charge of the membrane is zero. Following ^{31}P NMR experiments, Scherer and Seelig (1989) have proposed that the incorporation of a sublayer of positive charges below the phosphocholine moiety would tend to push away the positive choline group toward the aqueous medium, as a result of electrostatic repulsion, leading to an extended orientation of the choline segment almost perpendicular to the bilayer surface. The amplitude of the variations of the PC headgroup quadrupolar splittings observed in positively charged membranes would then be directly related to the magnitude of this conformational change of the choline headgroup. This conformational change of the PC headgroup can be viewed in our model by assigning the direction of the torque τ to the C–O bond of the glycerophosphocholine moiety [see Figure 7 of Scherer and Seelig (1989)]. According to our model, this torque should be reduced if part of the charges are located at the level of the $N^+(CH_3)_3$ choline group ($z_k \approx z$), and show an important increase in the width of the distribution (W_k) along the bilayer normal, as presumed for the charges of K^+ and pentalysine, leading then to weak changes of the quadrupolar splittings as observed with these two molecules. We suggest that fundamental theories of the type reviewed in the previous section be used to calculate the torque on PC and PS headgroups directly using a realistic model for the charge distribution in the headgroup [see, e.g., Gresh and Pullman (1980)] as well as in the aqueous medium.

A molecular picture of the charge-induced perturbation of the PS headgroup is hindered by the fact that, unlike that of the choline headgroup, the conformation of the serine moiety is at this time not known. Besides, the charge distribution of the PS headgroup is more intricate than that of the PC headgroup, since the phosphoserine moiety contains three charged functional groups (phosphate, amine, and carboxyl) as opposed to two for the phosphocholine headgroup (phosphate and choline). However, a potential clue in the understanding of the conformation of the PS headgroup in lipid membranes is provided by a very singular outcome of the ^2H NMR data obtained with headgroup-deuteriated PS. In DMPC/DMPS/$K_2GL_{20}K_2A$ 5:1:*X* membranes, the quadrupolar splitting of one of the serine α-methylene CD bonds, α_2, of DMPS hardly changes over a wide range of charge density, while the other, α_1, associated with the other *gem*-α-CD bond, i.e., borne by the *same* α-carbon of the serine, displayed important variations. This phenomenon has led us to assume that the serine headgroup undergoes a conformational change characterized by a rotation about a direction parallel to that of the CD bound associated with the nonperturbed splitting (Roux et al., 1989). It is interesting to note that the charge-induced choline headgroup rotation described by Scherer and Seelig (1989) occurs around the C–O bond of the glycerophosphocholine moiety, which is almost *parallel* to one of the α-CD bonds of the headgroup. Thus, it turns out that the ^2H NMR data obtained with the α-deuterons of the PS headgroup could be explained by a model related to that described by Scherer and Seeling (1989), provided that the parallel orientation of the headgroup α_2-deuteron and the C–O bond around which the torque is presumed to occur is conserved in the serine headgroup. In unsaturated POPC/POPS 5:1 membranes, incorporation of the peptide $K_2GL_{20}K_2A$ leads to results which are very similar to those observed in related saturated DMPC/DMPS 5:1 membranes, although a small decrease of the PS α_2 splitting is detected for the former. This result would indicate that the model described above is also valid for the POPC/POPS 5:1 membranes, with the difference that for POPS the α_2-CD bond would be less parallel to the C–O bond which we have assumed to be the axis of the charge-induced rotation of the serine headgroup. At low $CaCl_2$, $MgCl_2$, or LiCl concentrations, the α_2 splitting of the serine headgroup also displays a small decrease, correlated with the large changes of the two other serine splittings, suggesting that the conformational change undergone by the POPS headgroup can be also related to that discussed above. However, the sign reversal of the POPS α_2 splitting observed at higher salt levels, together with the plateauing values of the α_1 and β splittings, indicates that another kind of serine perturbation occurs under such conditions.

A detailed quantitative analysis of the PS headgroup ^2H NMR results, and complementary ^{31}P, ^{14}N, and ^{15}N NMR data, should allow a more precise determination of the conformational change of the serine headgroup induced by the presence of positive charges at the surface of PS-containing membranes.

Acknowledgments

We thank Professor Pieter Cullis and Elliott Burnell for generously providing us with various laboratory facilities required for the preparation of the materials used in this study. We thank Paulette Hervé for her participation in deuteriated lipid synthesis and Robert S. Hodges for providing us with the amphiphilic peptide $K_2GL_{20}K_2A$. We also thank Grenfell Patey for helpful discussions. The figures in this paper were prepared by using the computer graphics software developed at the Tri-University of Meson Facility (Vancouver, BC).

Registry No. POPC, 26853-31-6; POPS, 79980-16-8; Ca, 7440-70-2; Mg, 7439-95-4; Li, 7439-93-2; Na, 7440-23-5; K, 7440-09-7; serine, 56-45-1; choline, 62-49-7.

References

Altenbach, C., & Seelig, J. (1984) *Biochemistry 23*, 3913–3920.

Bentz, J., Düzgünes, N., & Nir, S. (1983) *Biochemistry 22*, 3320–3330.

Bentz, J., Alford, D., Cohen, J., & Düzgünes, N. (1988) *Biophys. J. 53*, 593–607.

Bitbol, M., Dempsey, C., Watts, A., & Devaux, P. F. (1989) *FEBS Lett. 244*, 217–222.

Bloch, J. M., & Yun, W. B. (1990) *Phys. Rev. A. 41*, 844–862.

Browning, J. L., & Seelig, J. (1980) *Biochemistry 19*, 1262–1270.

Büldt, G., Gally, H. U., Seelig, A., Seelig, J., & Zaccai, G. (1978) *Nature (London) 271*, 182–184.

Cevc, G., Seddon, J. M., & Marsh, D. (1985) *Biochim. Biophys. Acta 814*, 141–150.

Davis, J. H. (1979) *Biophys. J. 27*, 339–358.

Davis, J. H., Jeffrey, K. R., Bloom, M., Valic, M. I., & Higgs, T. P. (1976) *Chem. Phys. Lett. 44*, 390–394.

Davis, J. H., Clare, D. M., Hodges, R. S., & Bloom, M. (1983) *Biochemistry 22*, 5298–5305.

Dempsey, C., Bitbol, M., & Watts, A. (1989) *Biochemistry 28*, 6590–6596.

Eisenberg, M., Gresalfi, T., Riccio, T., & McLaughlin, S. (1979) *Biochemistry 18*, 5213–5223.
Feigenson, G. W. (1986) *Biochemistry 25*, 5819–5825.
Gresh, N., & Pullman, B. (1980) in *Biomolecular Structure, Conformation, Function and Evolution* (Srinivasan, R., Ed.) Vol. II, pp 575–584, Pergamon Press, Oxford and New York.
Hope, M. J., & Cullis, P. R. (1980) *Biochim. Biophys. Acta 92*, 846–852.
Kuchinka, E., & Seelig, J. (1989) *Biochemistry 28*, 4216–4221.
Lis, L. J., Lis, W. T., Parsegian, V. A., & Rand, R. P. (1981) *Biochemistry 20*, 1771–1777.
Macdonald, P. M., & Seelig, J. (1987a) *Biochemistry 26*, 1231–1240.
Macdonald, P. M., & Seelig, J. (1987b) *Biochemistry 26*, 6292–6298.
McLaughlin, S. (1989) *Annu. Rev. Biophys. Biophys. Chem. 18*, 113–136.
McLaughlin, S., Mulrine, N., Gresalfi, T., Vaio, G., & McLaughlin, A. (1981) *J. Gen. Physiol. 77*, 445–473.
Ninham, B. W. (1989) *Chem. Scr. 29A*, 15–21.
Patey, G. N., & Torrie, G. M. (1989) *Chem. Scr. 29A*, 39–47.
Pearson, R. H., & Pascher, I. (1979) *Nature (London) 281*, 499–501.
Portis, A., Newton, C., Pangborn, W., & Papahadjopoulos, D. (1979) *Biochemistry 18*, 780–790.
Roux, M., & Neumann, J. M. (1986) *FEBS Lett. 199*, 33–38.
Roux, M., Huynh-Dinh, T., Igolen, J., & Prigent, Y. (1983) *Chem. Phys. Lipids 33*, 41–45.
Roux, M., Neumann, J. M., Bloom, M., & Devaux, P. F. (1988) *Eur. Biophys. J. 16*, 267–273.
Roux, M., Neumann, J. M., Hodges, R. S., Devaux, P. F., & Bloom, M. (1989) *Biochemistry 28*, 2313–2321.
Scherer, P. G., & Seelig, J. (1987) *EMBO J. 6*, 2915–2922.
Scherer, P. G., & Seelig, J. (1989) *Biochemistry 28*, 7720–7728.
Seelig, A., Allegrini, P. R., & Seelig, J. (1988) *Biochim. Biophys. Acta 939*, 267–276.
Seelig, J., Macdonald, P. M., & Scherer, P. G. (1987) *Biochemistry 26*, 7535–7541.
Söderman, O., Arvidson, G., Lindblom, G., & Fontell, K. (1983) *Eur. J. Biochem. 134*, 309–314.
Sternin, E. (1985) *Rev. Sci. Instrum. 56*, 2043–2049.
Sternin, E., Bloom, M., & MacKay, A. L. (1983) *J. Magn. Reson. 55*, 274–282.
Tilcock, C. P. S., Bally, M. B., Farren, S. B., Cullis, P. R., & Gruner, S. M. (1984) *Biochemistry 23*, 2696–2703.
Torrie, G. M., Kusalik, P. G., & Patey, G. N. (1989) *J. Chem. Phys. 91*, 6367–6375.

Isolation and Characterization of a Novel Eukaryotic Monofunctional NAD$^+$-Dependent 5,10-Methylenetetrahydrofolate Dehydrogenase†

Charles K. Barlowe and Dean R. Appling*

Department of Chemistry and Clayton Foundation Biochemical Institute, The University of Texas, Austin, Texas 78712

Received February 27, 1990; Revised Manuscript Received April 16, 1990

ABSTRACT: An NAD$^+$-dependent 5,10-methylenetetrahydrofolate (THF) dehydrogenase has been purified to homogeneity from the yeast *Saccharomyces cerevisiae*. The purified enzyme exhibits a final specific activity of 5.4 units mg^{-1} and is represented by a single protein of apparent M_r = 33 000–38 000 as determined by sodium dodecyl sulfate gel electrophoresis. A native M_r = 64 000 was determined by gel filtration, suggesting a homodimer subunit structure. Cross-linking experiments with dimethyl suberimidate confirmed the dimeric structure. The enzyme is specific for NAD$^+$ and is not dependent on Mg^{2+} for activity. The forward reaction initial velocity kinetics are consistent with a sequential reaction mechanism. With this model, K_m values for NAD$^+$ and (6*R*,*S*)-5,10-methylene-THF are 1.6 and 0.06 mM, respectively. In contrast to all other previously described eukaryotic 5,10-methylene-THF dehydrogenases, the purified enzyme is apparently monofunctional, with undetectable 5,10-methenyl-THF cyclohydrolase and 10-formyl-THF synthetase activities. Subcellular fractionation of yeast indicates the enzyme is cytoplasmic, with no NAD$^+$-dependent 5,10-methylene-THF dehydrogenase detectable in mitochondria. The activity was found in all yeast strains examined, at all stages of growth from the lag phase through the stationary phase.

Folate-mediated one-carbon metabolism plays an essential role in several major cellular processes including nucleic acid biosynthesis, mitochondrial and chloroplast protein biosynthesis, amino acid biosynthesis and conversions, and vitamin metabolism. The variety of pathways that utilize these one-carbon units is dependent upon the ability of the organism to vary the oxidation state of the carbon unit attached to the coenzyme, tetrahydrofolate (THF).[1] In most organisms, the major source of one-carbon units is the 3-carbon of serine, derived from glycolytic intermediates (Schirch, 1978). The one-carbon unit is transferred to THF in a reaction catalyzed

†Supported by the Foundation for Research and by NIH Grant DK-36913.

[1] Abbreviations: THF, tetrahydrofolate; Tris, tris(hydroxymethyl)-aminomethane; SDS–PAGE, sodium dodecyl sulfate–polyacrylamide gel electrophoresis; EDTA, ethylenediaminetetraacetic acid; K-HEPES, *N*-(2-hydroxyethyl)piperazine-*N*′-2-ethanesulfonic acid potassium salt; PMSF, phenylmethanesulfonyl fluoride.

0006-2960/90/0429-7089$02.50/0